

Supplementary Tables

Supplementary Table 1. Targeted drug screen candidates for PI3K/Akt combination treatments and respective inhibited pathways.

Inhibitor	Target	Inhibitor	Target
Onipalisib	PI3K α / β / δ / γ	Mebendazole	Tubulin depolymerization
		Ibrutinib	Brutons tyrosine kinase BTK & ITK
		Crizotinib	Multi-tyrosine kinase, c-MET
		PF-3758309	PAK4
		KPT-9274	PAK4 and NAMPT
		(-)- β -Hydrastine	PAK4
Pictilisib	PI3K α / δ	PF-3758309	PAK4
Buparlisib	PI3K α / β / δ / γ	Danusertib	Aurora-A/B/C Kinase
		Nintedamib	WGFR-1/2/3
		Crizotinib	Multi-tyrosine kinase, c-MET
		PF-3758309	PAK4
		KPT-9274	PAK4 and NAMPT
		(-)- β -Hydrastine	PAK4

Supplementary Table 2. EC50 drug concentrations for human (HS01, HS02/HS03) and mouse (MS01) MD-SC lines when drugs are delivered as monotherapies.

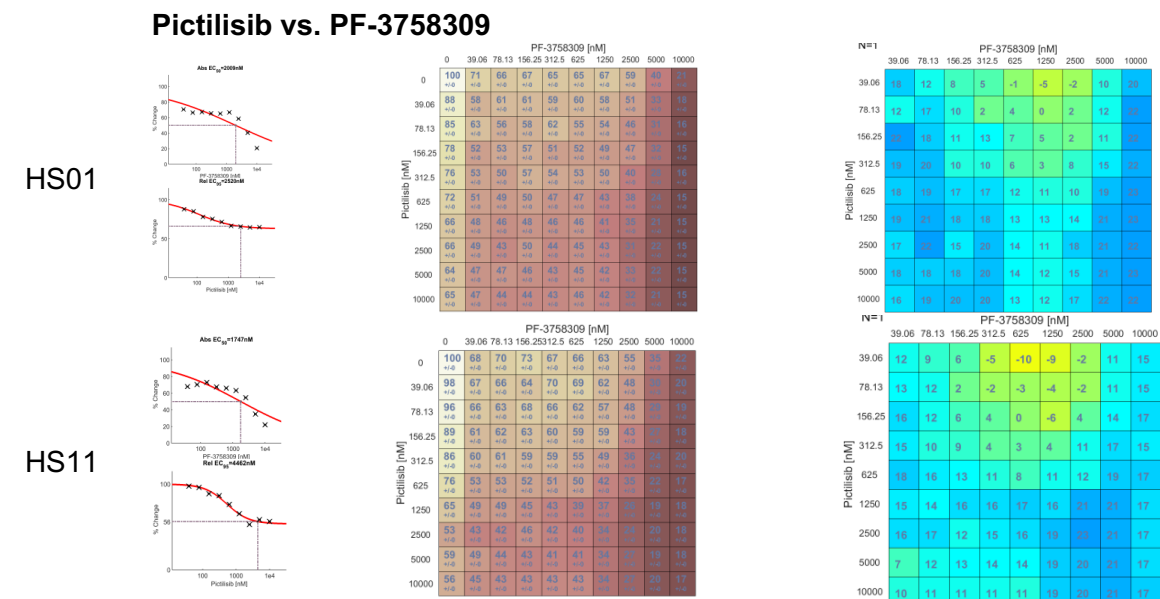
Inhibitor	EC50 HS01	EC50 HS02/HS03	EC50 MS01
Onipalisib	2.02 nM	26.8 nM	7.01 nM
Pictilisib	> 10 μ M	> 10 μ M	1462 nM
Buparlisib	1905 nM	2098 nM	870 nM
Mebendazole	2068 nM	774 nM	195 nM
Ibrutinib	7812 nM	11.7 μ M	7045 nM
Crizotinib	1536 nM	621 nM	
PF-3758309	2009 nM	1765 nM	207 nM
KPT-9274	> 10 μ M	691 nM	
(-)- β -Hydrastine	> 10 μ M	384 nM	
Danusertib	1527 nM	15.6 μ M	9071 nM
Nintedamib	5352 nM	> 10 μ M	3121 nM

Supplementary Table 3. Loewe synergy scores (sum_syn_ant) for drug combinations in human MD-SC lines (HS01, HS03) and mouse MD-SC lines (MS01). Drugs were tested in 10x10 combination matrices.

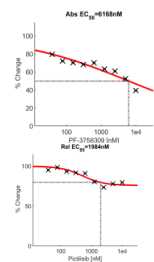
Inhibitor	Inhibitor	Loewe Synergy Score (HS01)	Loewe Synergy Score (HS03)	Loewe Synergy Score (MS01)
Ompalisib	Mebendazole	16.49	3.25	2.53
	Ibrutinib	12.65	1.02	3.27
	Crizotinib	12.12	7.02	
	PF-3758309	73.55	12.12	
	KPT-9274	1.00	6.89	
	(-)- β -Hydrastine	8.42	43.60	
Pictilisib	PF-3758309	79.75	58.85	93.12
Buparlisib	Danusertib	28.4	12.06	1.99
	Nintedamib	4.27	43.69	7.76
	Crizotinib	9.44	4.79	
	PF-3758309	36.66	9.44	
	KPT-9274	33.47	28.06	
	(-)- β -Hydrastine	1.46	9.44	

Supplementary Figures

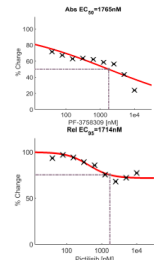
Supplementary Figure S1



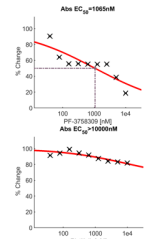
HS04.3



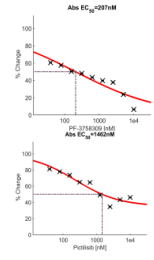
HS03



HS12

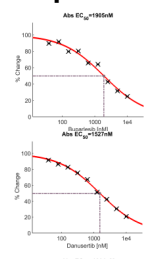


MS01

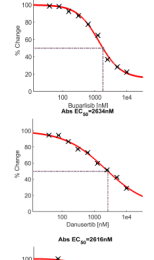


Buparlisib vs. Danusertib

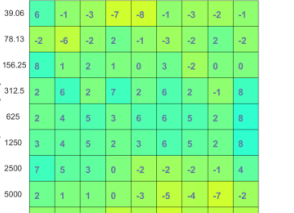
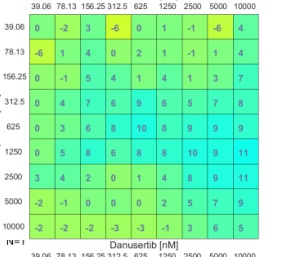
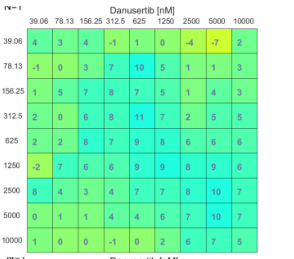
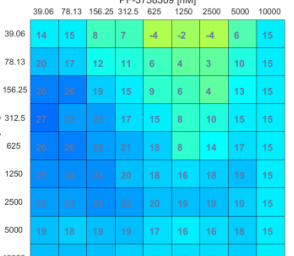
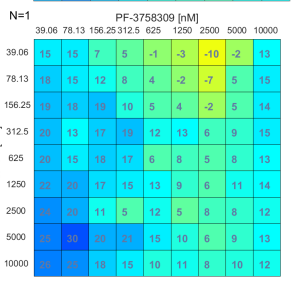
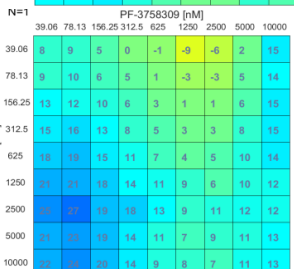
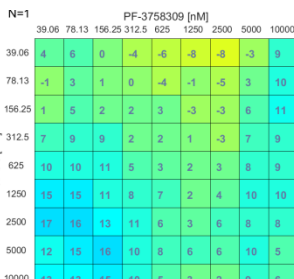
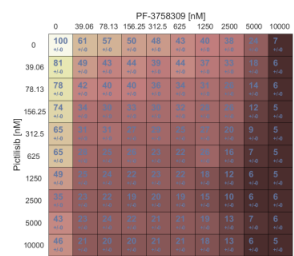
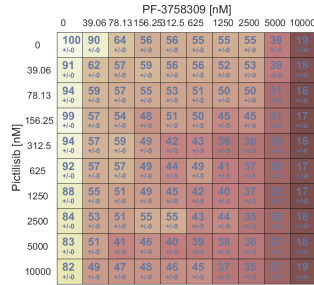
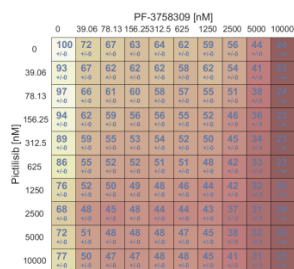
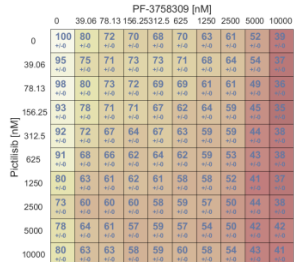
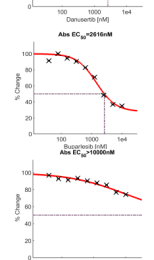
HS01



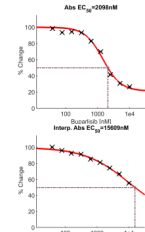
HS11



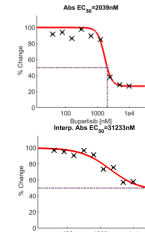
HS04.3



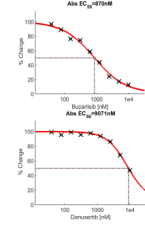
HS03



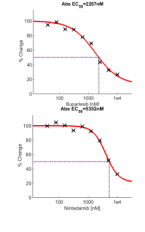
HS12



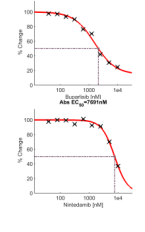
MS01



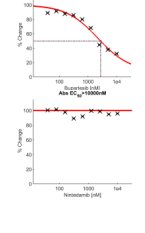
HS01



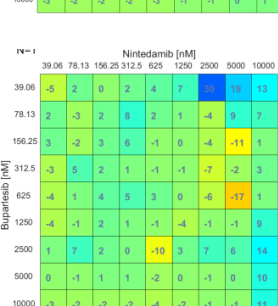
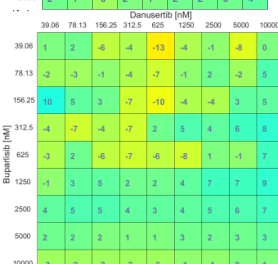
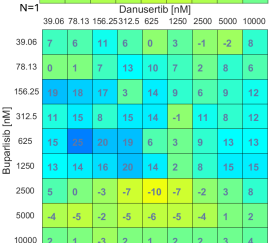
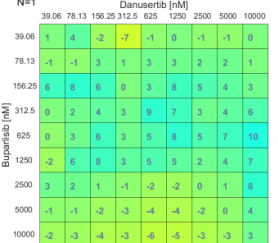
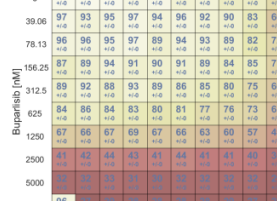
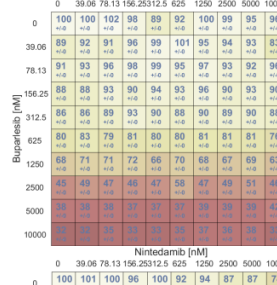
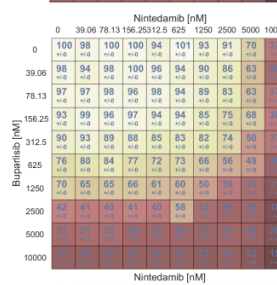
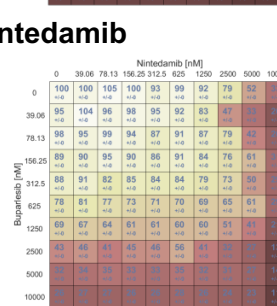
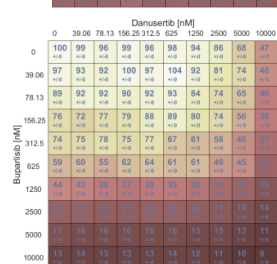
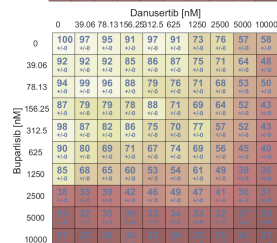
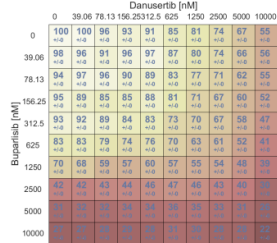
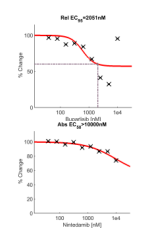
HS11



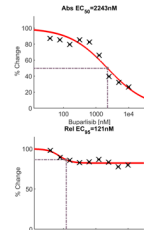
HS04.3



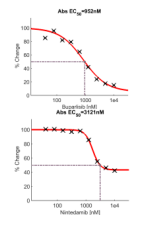
HS03



HS12

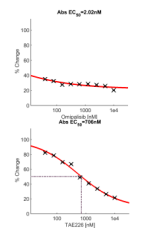


MS01

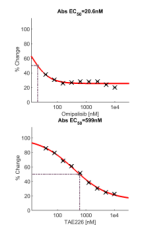


Omipalisib vs. TAE226

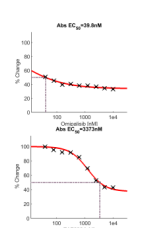
HS01



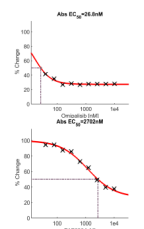
HS11



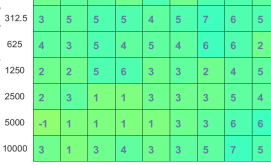
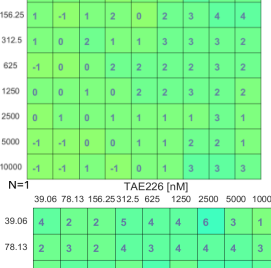
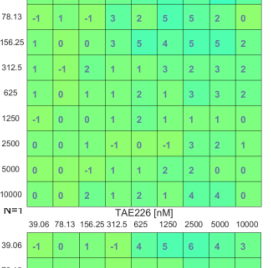
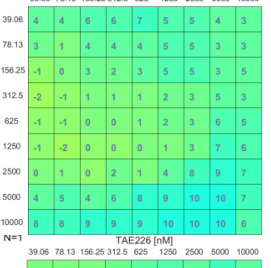
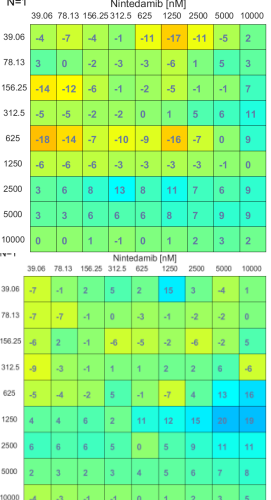
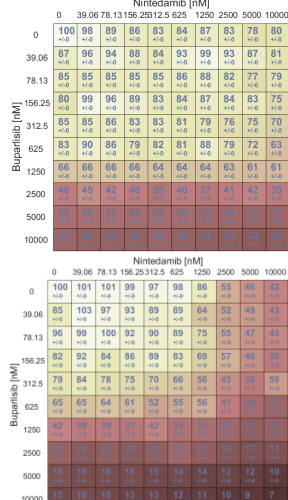
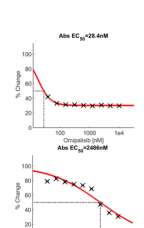
HS04.3



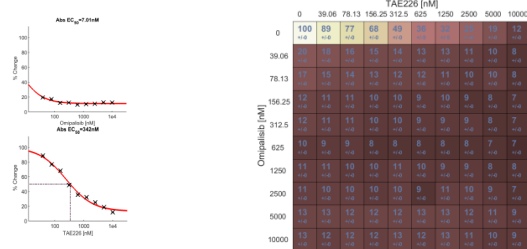
HS03



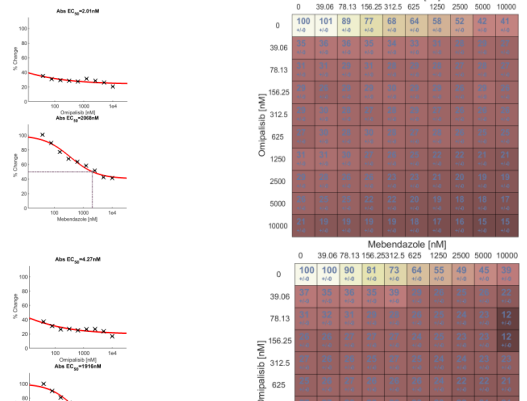
HS12



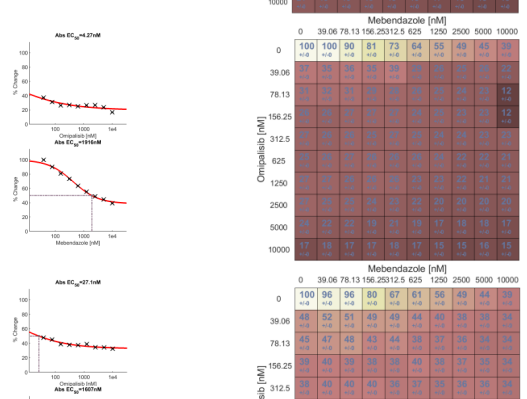
MS01



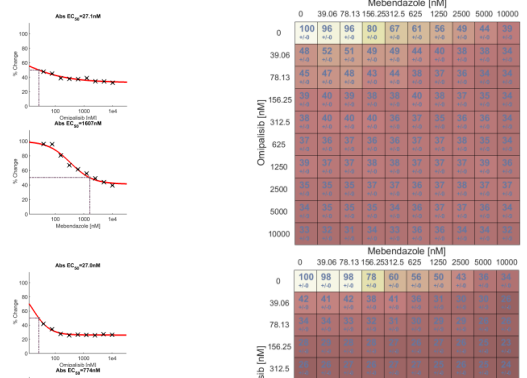
HS01



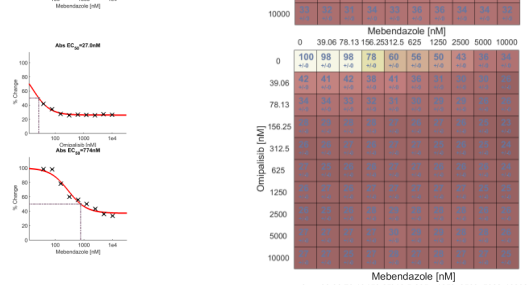
HS11



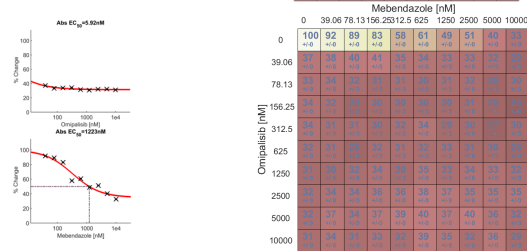
HS04.3



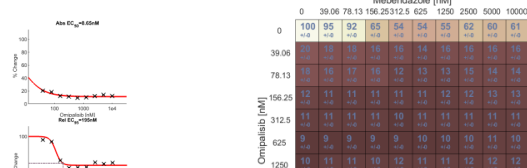
HS03



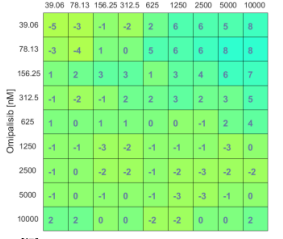
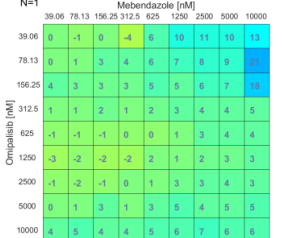
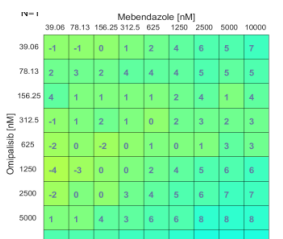
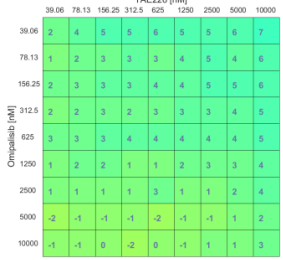
HS12



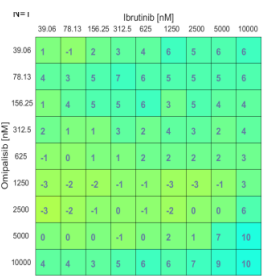
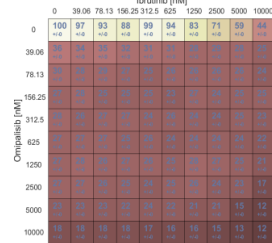
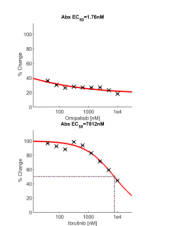
MS01



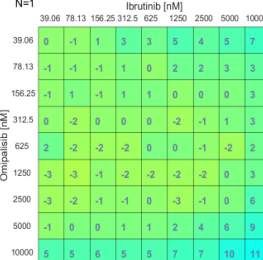
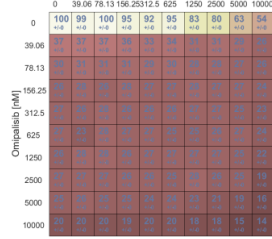
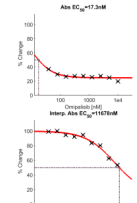
Omipalsib vs. Ibrutinib



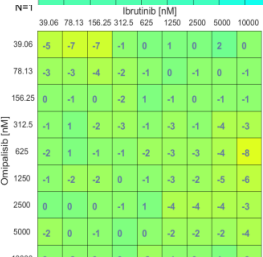
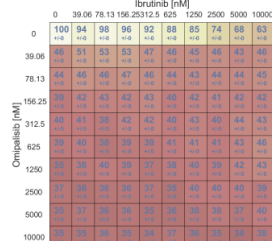
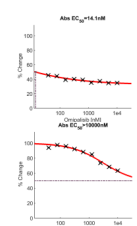
HS01



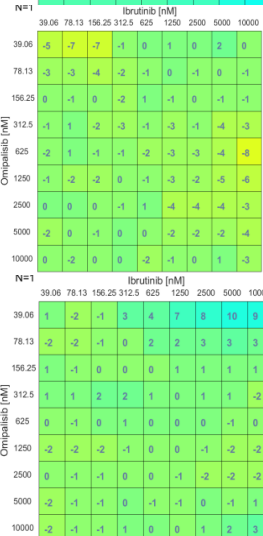
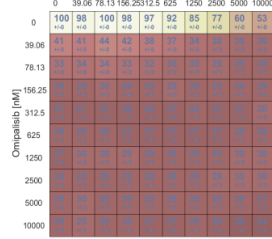
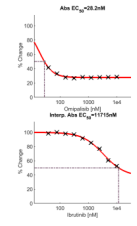
HS11



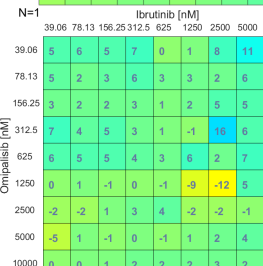
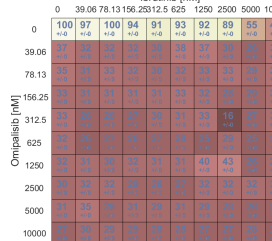
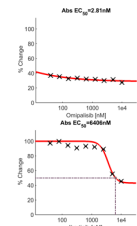
HS04.3



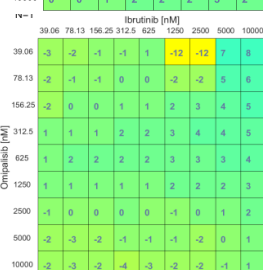
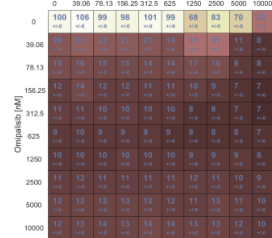
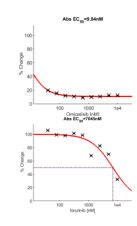
HS03



HS12



MS01

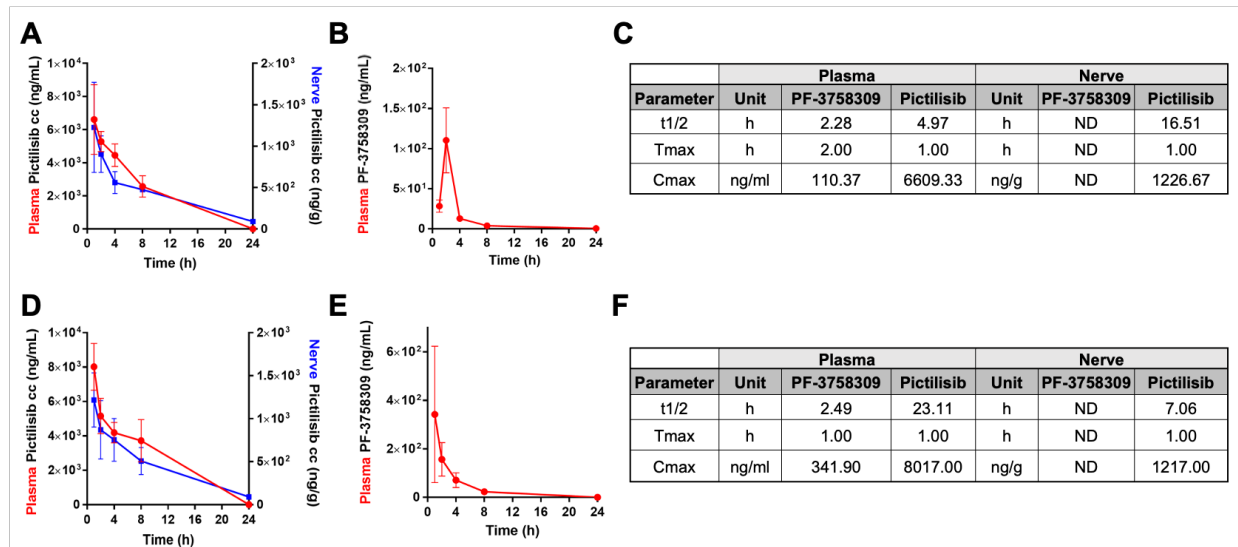


Viability

Loewe synergy and antagonism

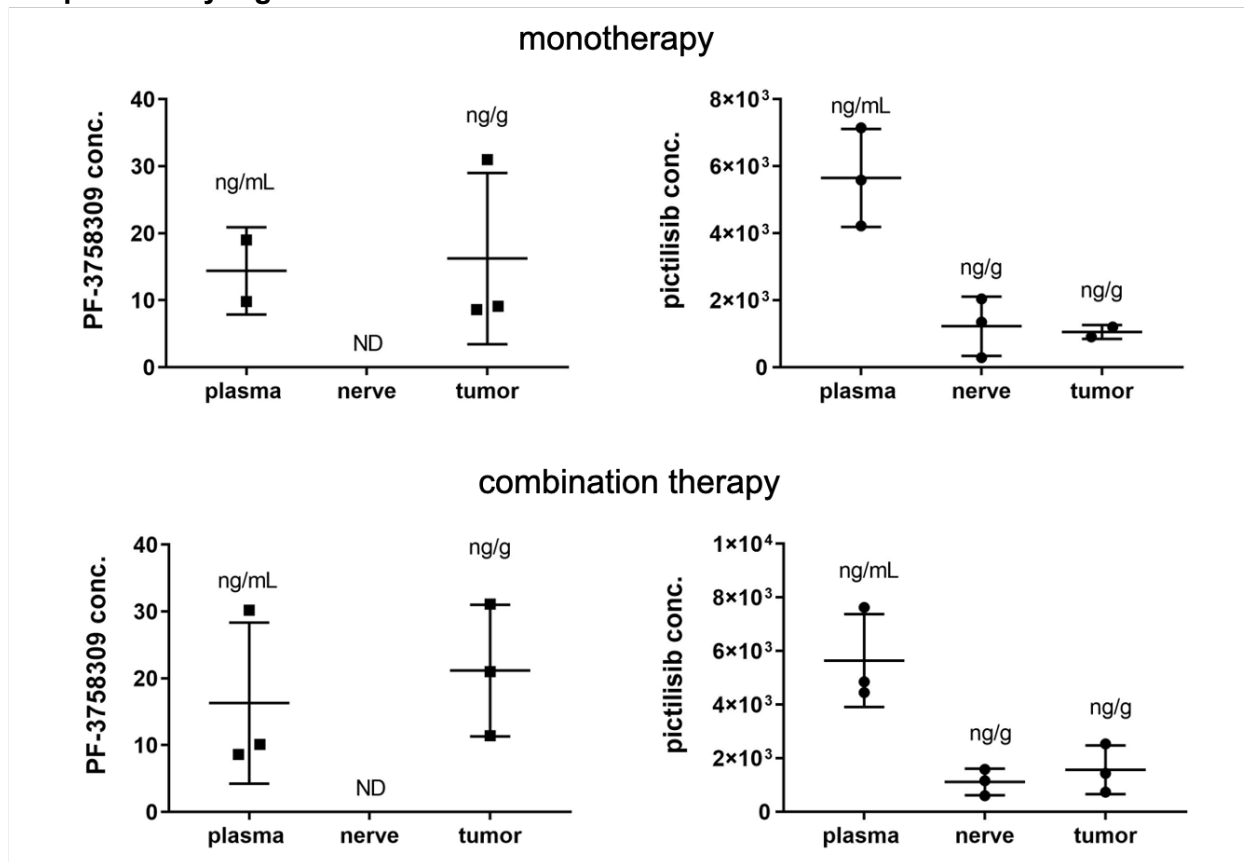
Supplementary figure S1. Data from cell cytotoxic assays for tested inhibitors in combinations by cell line: MS01 - mouse MD-SC line, HS01 – human MD-SC line (shRNA knock down), HS11 - human SC line, HS04.3 - human monoclonal MD-SC line (CRISPR/Cas9 knock out), HS03 - human MD-SC line (CRISPR/Cas9 knock out), HS12 - human Sc line.

Supplementary Figure S2



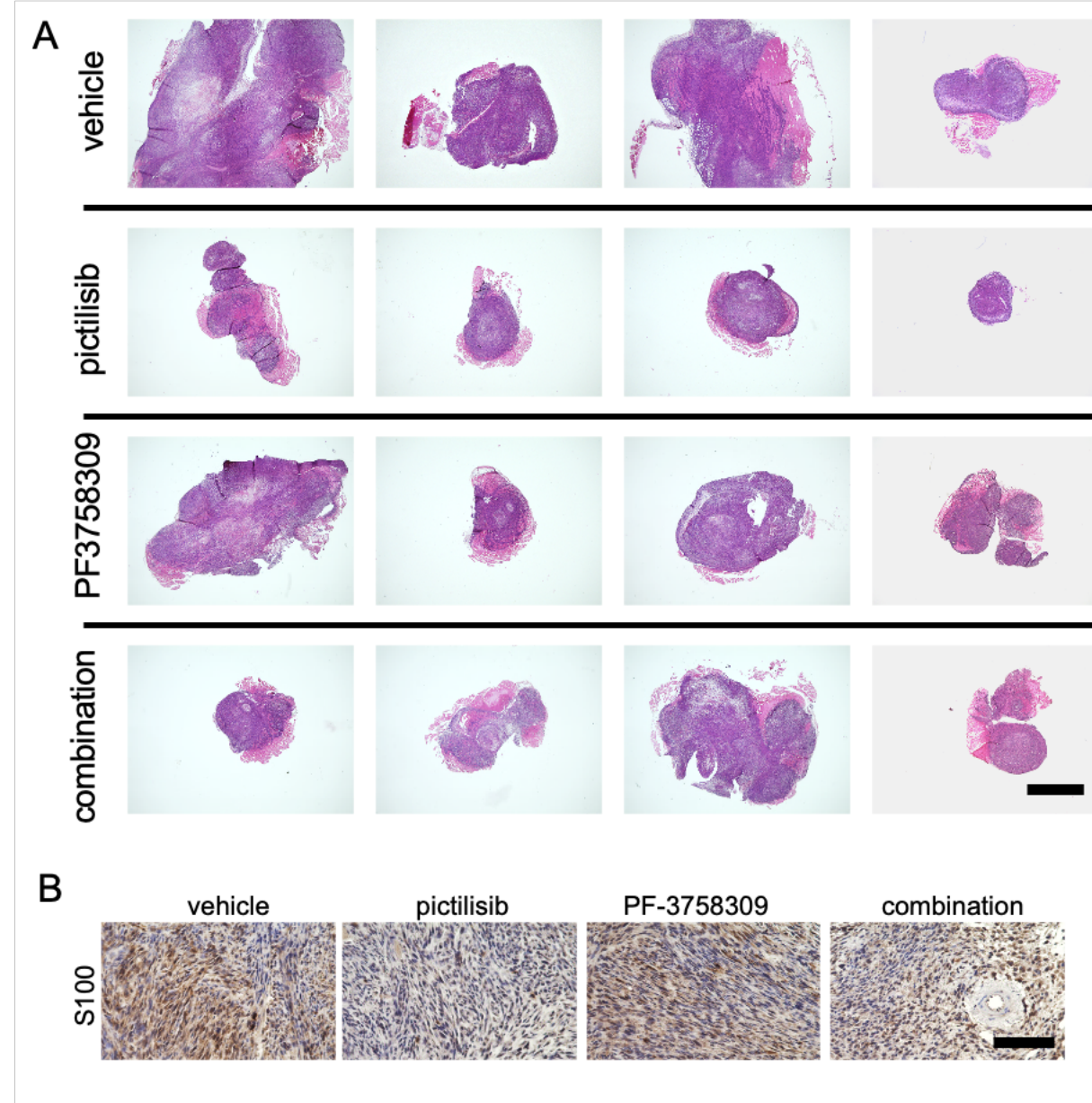
Supplementary Figure S2. Pharmacokinetic analysis of pictilisib and PF-3758309 as monotherapies and in combination after a single dose. (A) Plot of monotherapeutic pictilisib concentration as a function of time (plasma shown in red, nerve shown in blue). (B) Plot of monotherapeutic PF-3758309 concentration in plasma as a function of time (not detected in nerve). (C) Pictilisib and PF-3758309 pharmacokinetic parameters when delivered as monotherapeutics. (D) Plot of pictilisib concentration in the presence of PF-3758309 as a function of time (plasma shown in red, nerve shown in blue). (E) Plot of PF-3758309 concentration in plasma in the presence of pictilisib as a function of time (not detected in nerve). (F) Pictilisib and PF-3758309 pharmacokinetic parameters when delivered in combination. Data in graphs shown as mean \pm SEM. t_{1/2}: plasma/nerve half-life; T_{max}: time to maximum plasma/nerve concentration; C_{max}: peak plasma/nerve concentration

Supplementary Figure S3



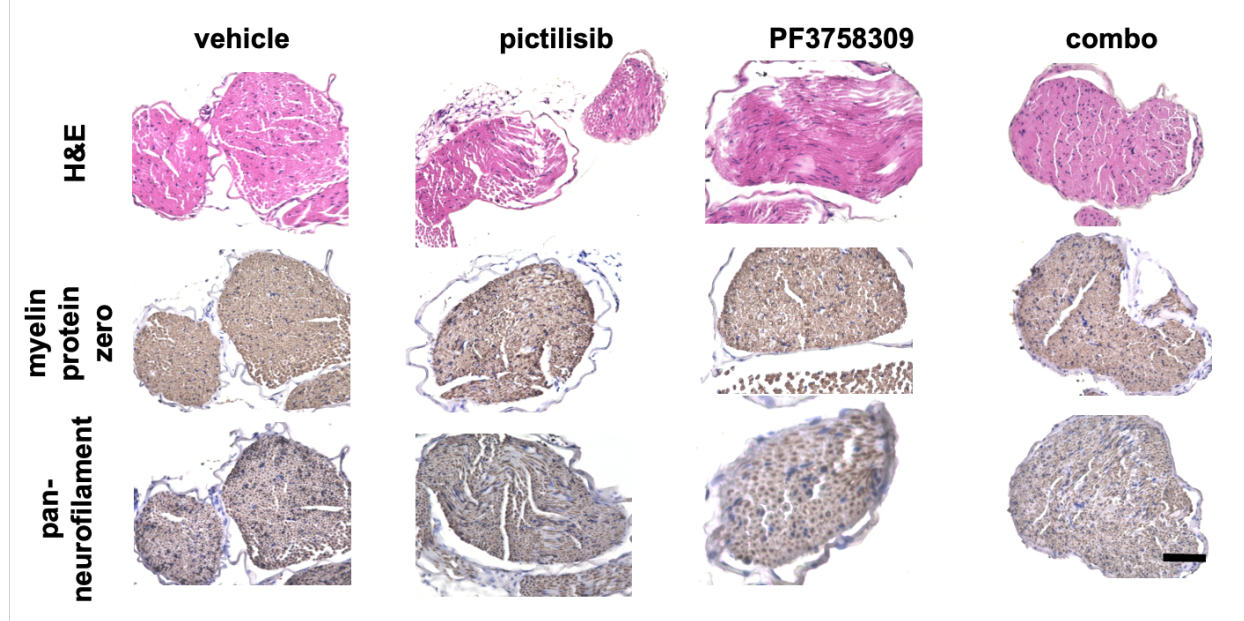
Supplementary Figure S3. Pharmacokinetic analysis of pictilisib and PF-3758309 as monotherapies and in combination after two weeks of daily dosing. PF-3758309, although not detected in naïve nerve, was detected in tumor, revealing disruption of the blood-nerve barrier in nerves grafted with the merlin-deficient Schwann cells and the possibility of reduced clearance rate from the tumors for PF-3758309. PF-3758309 was detected at similar levels in plasma and tumor when delivered alone and with pictilisib. Pictilisib was observed in the plasma, normal nerve and tumors of all mice treated as single or combination therapy.

Supplementary Figure S4



Supplementary Figure S4. Representative images of graft samples processed for histology (n=4/group) and (A) stained with hematoxylin and eosin imaged at 50x and (B) stained for S100 expression and imaged at 400x. Scale bar in A represents 1.5 mm. Scale bar in B represents 200 μ m.

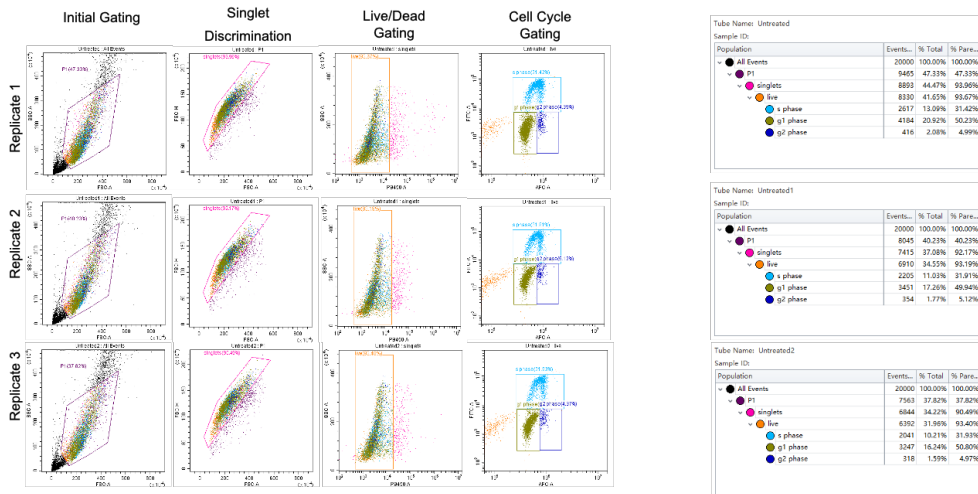
Supplementary Figure S5



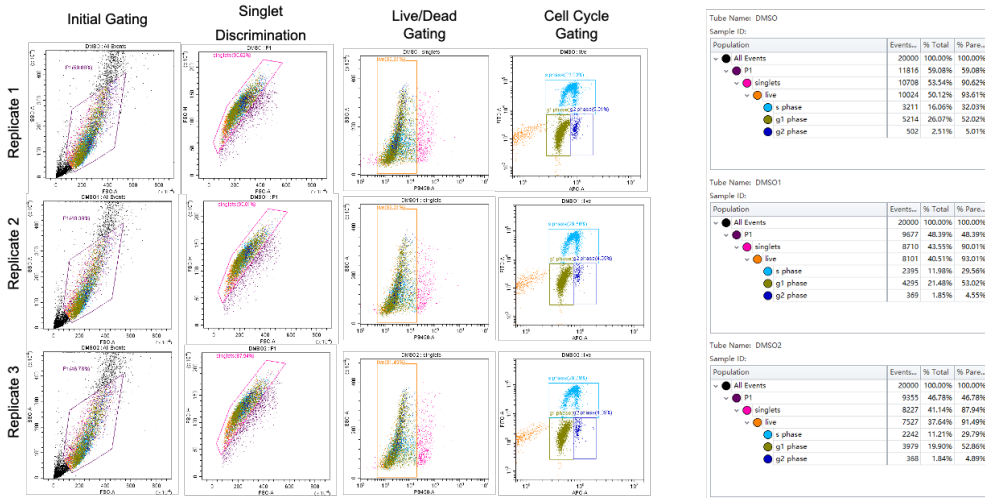
Supplementary Figure S5. Representative 100x images of contralateral control sciatic nerve samples processed for histology and stained with hematoxylin and eosin, myelin protein zero, and pan-neurofilament. There are no clear differences between groups in nerve morphology or Schwann cell-specific protein expression. Scale bar represents 400 μ m.

Supplementary Figure S6

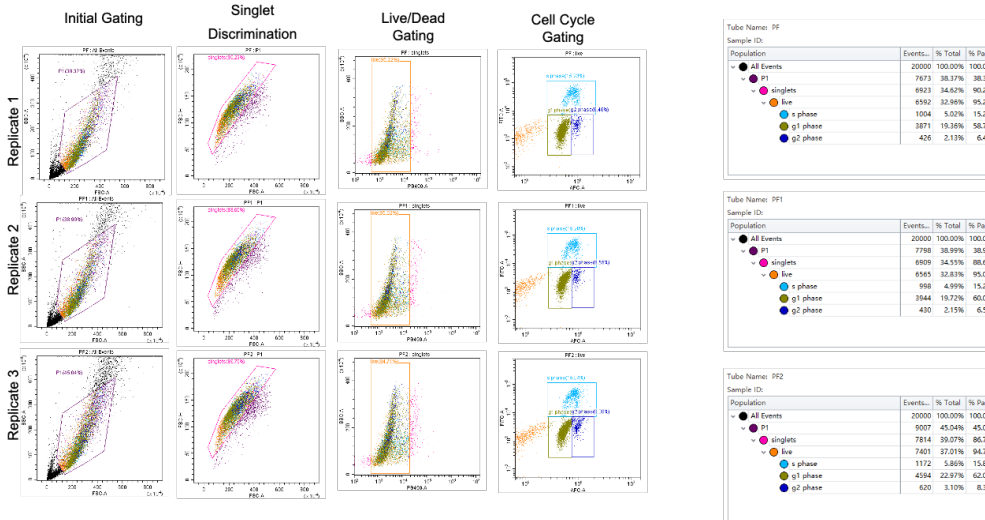
Untreated cells



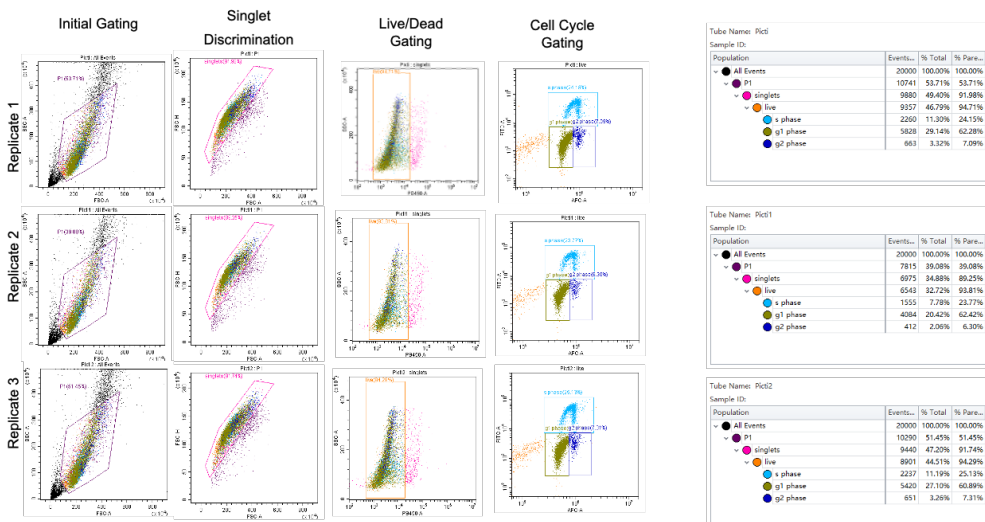
DMSO treated cells



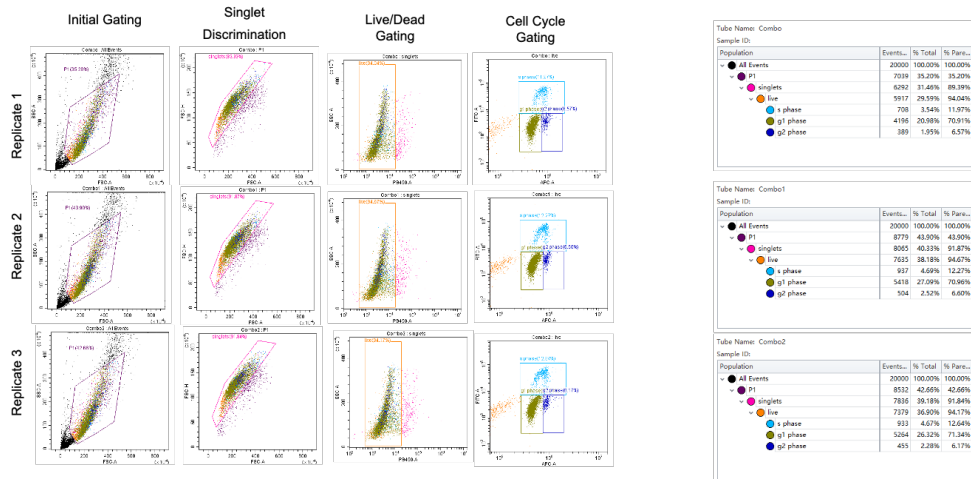
PF-3758309 treated cells



Pictilisib

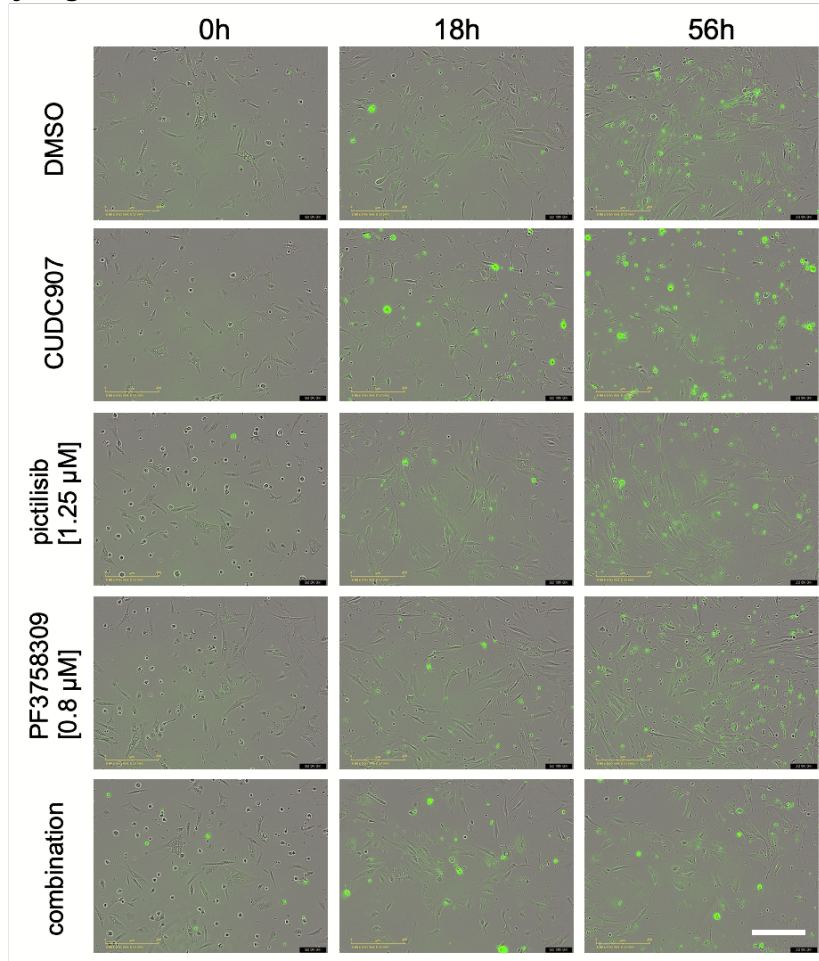


Combination treated cells



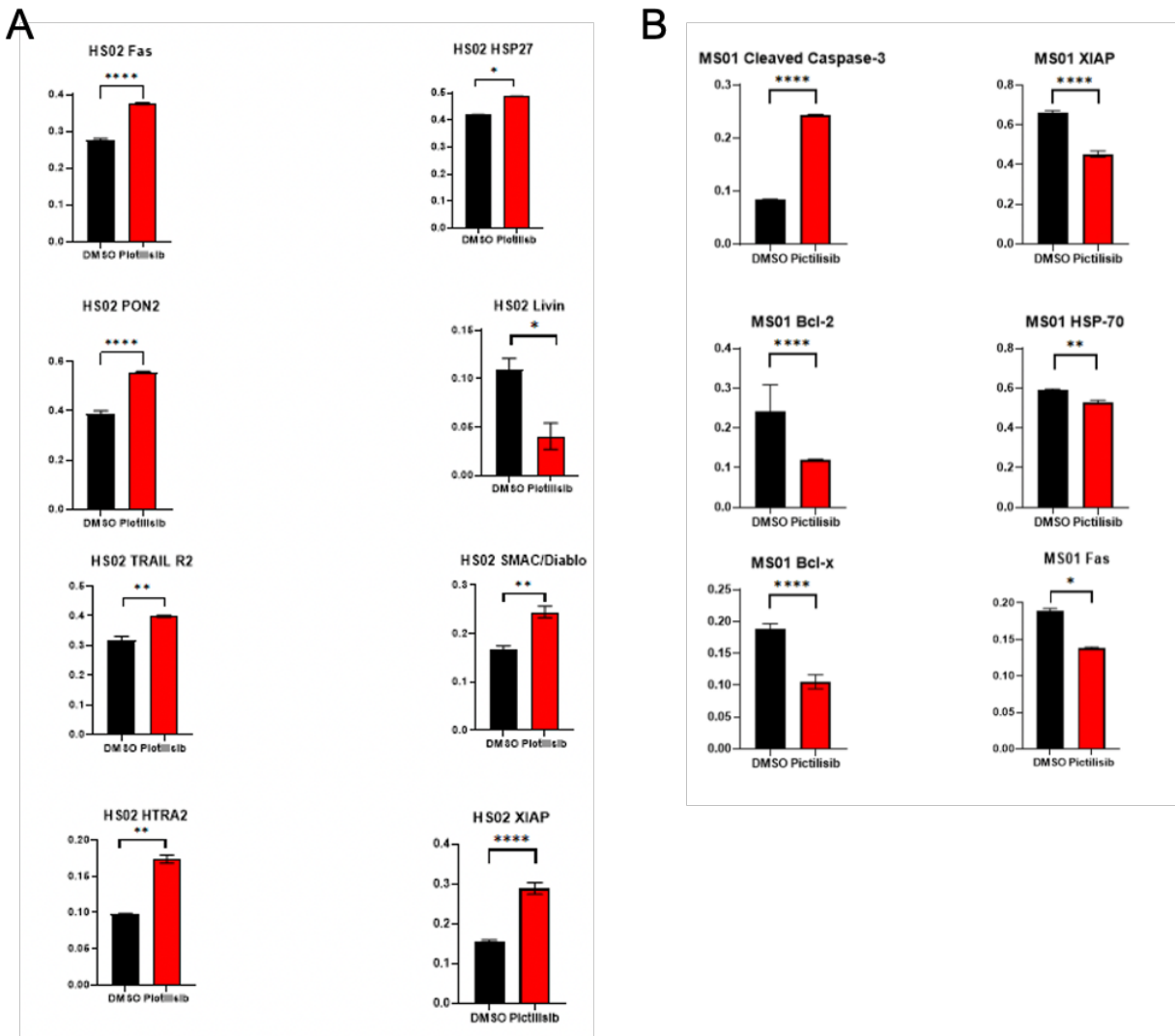
Supplementary Figure S6. Flow analysis of cell cycle in treated and untreated HS01 cells.

Supplementary Figure S7



Supplementary Figure S7. Representative images of cleaved caspase3/7+ (green) cells imaged at 0h, 18h, and 54h of cultures with indicated treatments.

Supplementary Figure S8.



Supplementary Figure S8. All significant differences in protein levels detected by human (A) and mouse (B) Apoptosis Proteome Profiles arrays. *p<0.05; **p<0.01, ****p<0.0001 by Šídák's multiple comparisons test.